RESPONSE OF BASE-ISOLATED USC HOSPITAL BUILDING IN NORTHRIDGE EARTHQUAKE

By Satish Nagarajaiah,[1] Member, ASCE, and Sun Xiaohong,[2] Associate Member, ASCE

ABSTRACT: The base-isolated University of Southern California (USC) hospital building experienced strong motion during the 1994 Northridge earthquake. California Strong Motion Instrumentation Program data of the response are available for performance evaluation. The objective of this study is to evaluate the seismic performance of the base-isolated USC hospital building during the 1994 Northridge earthquake. A nonlinear analytical model of the USC hospital building is developed and verified using system identification. The response computed, using the presented analytical modeling techniques, is verified using recorded data. Structural behavior during the Northridge earthquake is evaluated in detail. The base-isolated USC hospital building performed well and reduced the response when compared to a fixed-base structure. The free-field acceleration was 0.49*g* and peak foundation/ground acceleration was 0.37*g*. The peak roof acceleration was reduced to 0.21*g*, nearly 50% of the peak ground acceleration. The peak drift was <30% of the code specification. The bearings yielded and dissipated energy (20%). The superstructure was elastic due to the effectiveness of base isolation. The building is expected to perform well in future earthquakes similar to those used in the original design.

INTRODUCTION

Elastomeric isolation bearings are introduced between the superstructure and the foundation to provide lateral flexibility and energy dissipation capacity. The lateral flexibility leads to a fundamental period of the base-isolated structure that is much longer than both its fixed-base period and predominant periods of ground motion. The response is reduced due to this period shift and dominant fundamental mode response.

The recorded response of the base-isolated University of Southern California (USC) hospital in the 1994 Northridge earthquake (Shakal et al. 1994) is available for evaluation. The objective of this study is to evaluate the effectiveness of base isolation in reducing the response. Analytical modeling techniques for base-isolated structures are presented. A detailed 3D nonlinear analytical model of the USC hospital building is developed based on as-built structural details and prototype bearing test results. The actual dynamic characteristics of the building are estimated based on the identified and recorded transfer functions obtained from recorded input and output responses. The analytical model is verified by comparing the analytical and identified periods/damping ratios. Comparison between recorded and computed responses is presented. The accuracy of the analytical modeling techniques used in base-isolated structures is evaluated. Structural behavior during the Northridge earthquake is evaluated. The evaluations include comparison of the response of the base-isolated building with the probable response if the building were fixed base.

It is shown that the base-isolated USC hospital building performed to expectations and reduced the response when compared to a fixed-base structure. Recorded and computed responses, which support this fact, are presented.

BASE-ISOLATED USC HOSPITAL BUILDING

The USC hospital building is a base-isolated seven-story (seven stories above the ground and a basement), steel-braced framed building, 92.35-m (303-ft) long, and 77.11-m (253-ft) wide, with 10 bays in the east-west (EW) direction and 12 bays in the north-south (NS) direction. Fig. 1 shows the plan and elevation of the building. The floor plan is asymmetric with two wings, which are connected by a necked down region of the floor/base. The building has setbacks after the fifth floor. Metal decking and a grid of steel beams support all concrete floors. The superstructure bracing is located at the building perimeter. The steel superstructure is supported on a reinforced concrete base slab, which is integral with the reinforced concrete beams below, and drop panels below each column location. The isolators are connected between these drop panels and the footings below [Fig. 1(b)]. The footings also support a reinforced concrete pedestal provided for backup safety. The seismic isolation system consists of 68 lead-rubber isolators and 81 elastomeric isolators, as shown in Fig. 1.

The building is located near the intersection of Highways 5 and 10. The closest active faults to the site are the Raymond Fault and the Newport-Ingelwood Fault. The building was designed using spectrum compatible earthquakes—with the spectrum defined as 1.2 times the 0.4*g* ATC-3-06 or UBC spectrum [Fig. 2(b)] corresponding to a soil type of S1.

Lead-Rubber and Elastomeric Isolation System

The isolation system of the USC hospital building is made up of a combination of lead-rubber bearings (elastomeric bearing with lead core) and elastomeric bearings. The bearing distribution is shown in Fig. 1. The lead-rubber bearings support exterior columns, and the elastomeric bearings support interior columns. The isolation system consists of a total of 149 isolation bearings: 59 lead-rubber bearings, 55.88-cm (22-in.) square, with 13.97-cm (5.5-in.) diameter lead core; 9 lead-rubber bearings, 66.04-cm (26-in.) square, with 13.97-cm (5.5-in.) diameter lead core; 8 elastomeric bearings, 55.88-cm (22-in.) square; and 73 elastomeric bearings, 66.04-cm (26-in.) square. The isolators are made of natural rubber with a shear modulus of 100 psi at 50% strain. The steel shim plates are of nominal thickness, 0.31 cm (0.12 in.). Top and bottom cover plates are 2.54-cm (1-in.) thick. The total height of the bearings is 34.61 cm (13.625 in.), with 14 layers of rubber and 13 steel shim plates. The bearings are doweled into the end plates. Fig. 1(b) shows details of a typical isolation bearing with fail-safe concrete pedestals. The isolators are designed for a maximum displacement of 26.04 cm (10.25 in.). The prototype testing of the isolators has been performed by Dynamic Isolation Systems (DIS 1989).

Recorded Response in Northridge Earthquake

The building was instrumented by the California Strong Motion Instrumentation Program (CSMIP) (Shakal et al.

[1]Assoc. Prof., Dept. of Civ. Engrg., Rice Univ., Houston, TX 77005.
[2]Des. Engr., CBM Engineers, Houston, TX 77004.

Note. Associate Editor: Sashi Kunnath. Discussion open until March 1, 2001. To extend the closing date one month, a written request must be filed with the ASCE Manager of Journals. The manuscript for this paper was submitted for review and possible publication on May 17, 1999. This paper is part of the ***Journal of Structural Engineering***, Vol. 126, No. 10, October, 2000. ©ASCE, ISSN 0733-9445/00/0010-1177–1186/$8.00 + $.50 per page. Paper No. 21017.

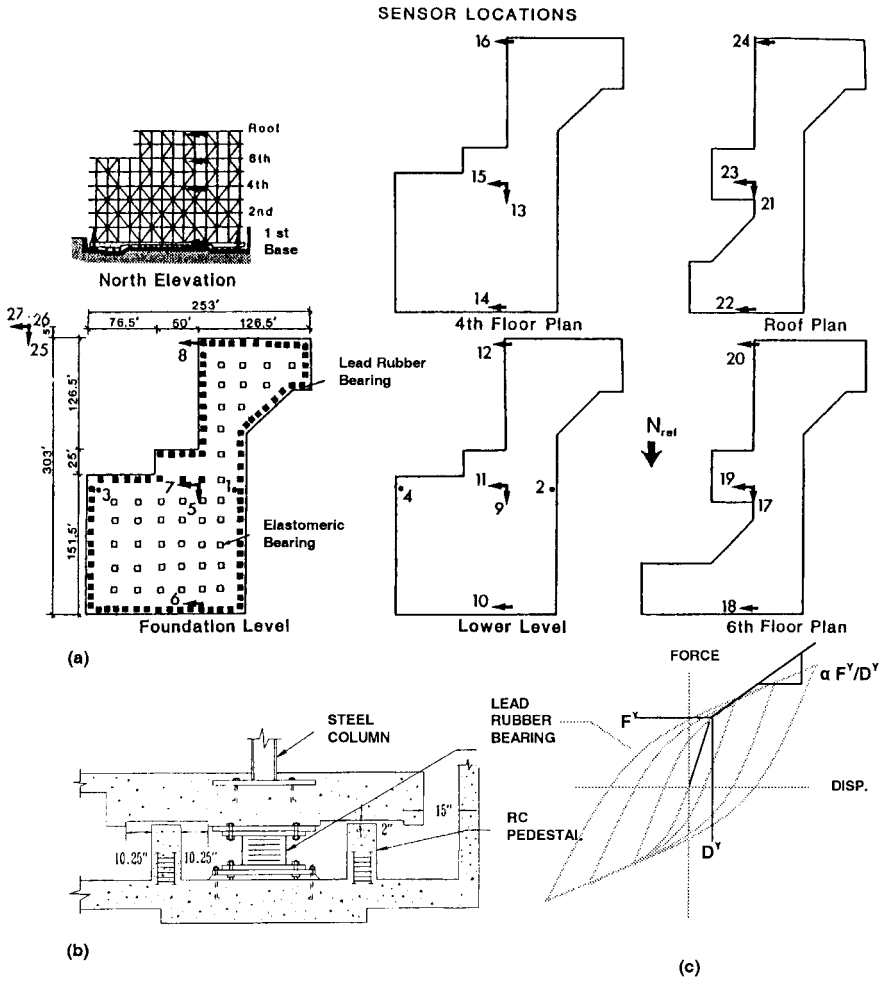

FIG. 1. USC Hospital Building (1 ft = 0.3048 m; 1 in. = 2.54 cm): (a) Elevation, Plan, Sensor Locations; (b) Isolation System Details; (c) Smooth Bilinear Hysteretic Force-Displacement Loops of Lead-Rubber Bearing

1994); the sensor locations are shown in Fig. 1. The sensors [accelerometers; here called channels (CHNs)] are centrally located at the foundation (CHN5 and CHN7), lower level or base (CHN9 and CHN11), fourth floor (CHN13 and CHN15), sixth floor (CHN17 and CHN19), and roof (CHN21 and CHN23) in the NS and EW directions. Sensors (CHN6/8, CHN10/12, CHN14/16, CHN18/20, and CHN22/24) are located at the east and west ends of the corresponding floors to measure lateral-torsional motions. Three sensors (CHN25, CHN26, and CHN27) are embedded in the ground to record the free-field ground motion. Sensors CHN1/3 and CHN2/4 measure the vertical response at the foundation level and lower or base level, respectively. The peak values of recorded absolute acceleration in the EW and NS directions during the Northridge earthquake are shown in Table 1. Evaluation of the recorded response is presented along with detailed analysis results later. The peak free-field acceleration of 0.49*g* occurred at CHN25 in the NS direction. The peak vertical acceleration at CHN3 was 0.09*g*, and at CHN4 it was 0.13*g*. The peak ground accelerations of 0.13*g*, 0.16*g*, and 0.17*g* occurred at CHN6, CHN7, and CHN8, respectively, in the EW direction. The recorded time histories of ground acceleration at CHN5–CHN8 are presented in Fig. 2. Examination of the CHN5 record indicates that a 0.4-s period acceleration pulse with peak ground acceleration 0.37*g* occurred between 16.2 and 16.6 s in the NS direction. The response spectra for 5% damping, presented in Fig. 2(b), show that the ground acceleration spectra for CHN 5–CHN8 are enveloped by 1.2 times 0.4*g* ATC-3-06 or UBC design spectrum for soil type S1. In the NS direction the spectral acceleration is comparable to the design spectrum for periods <0.5 s, but it is substantially smaller for periods >0.5 s. The spectra in the EW direction are well below the design spectrum.

3D NONLINEAR ANALYTICAL MODELING

Nonlinear analytical modeling techniques (Nagarajaiah et al. 1991b) used for dynamic analysis of the base-isolated USC hospital are presented briefly. The equations and parameters presented are relied on to explain the approach used in this study and to clarify the results of the study throughout the paper.

The localized nonlinearities at the isolation level allow condensation of the linear superstructure to a small number of master degrees of freedom (DOF). The superstructure and the base are modeled with 3 master DOF per floor at the center of mass. The base and floors are assumed to be infinitely rigid in plane. Each nonlinear elastomeric bearing at the isolation level is modeled explicitly using discrete biaxial elements, and the forces in the bearings are transformed to the center of mass of the base using the rigid base slab assumption. In addition, the equations of motion are developed in such a way that the fixed-base properties are used for modeling the linear superstructure. The equations of motion for the superstructure are as follows:

$$\mathbf{M}\ddot{\mathbf{u}} + \mathbf{C}\dot{\mathbf{u}} + \mathbf{K}\mathbf{u} = -\mathbf{M}\mathbf{R}(\ddot{\mathbf{u}}_g + \ddot{\mathbf{u}}_b) \quad (1)$$

where **M**, **C**, and **K** = superstructure mass, damping, and stiffness matrices, respectively, in the fixed-base condition; **R** = influence matrix; $\ddot{\mathbf{u}}$, $\dot{\mathbf{u}}$, and **u** represent the floor acceleration,

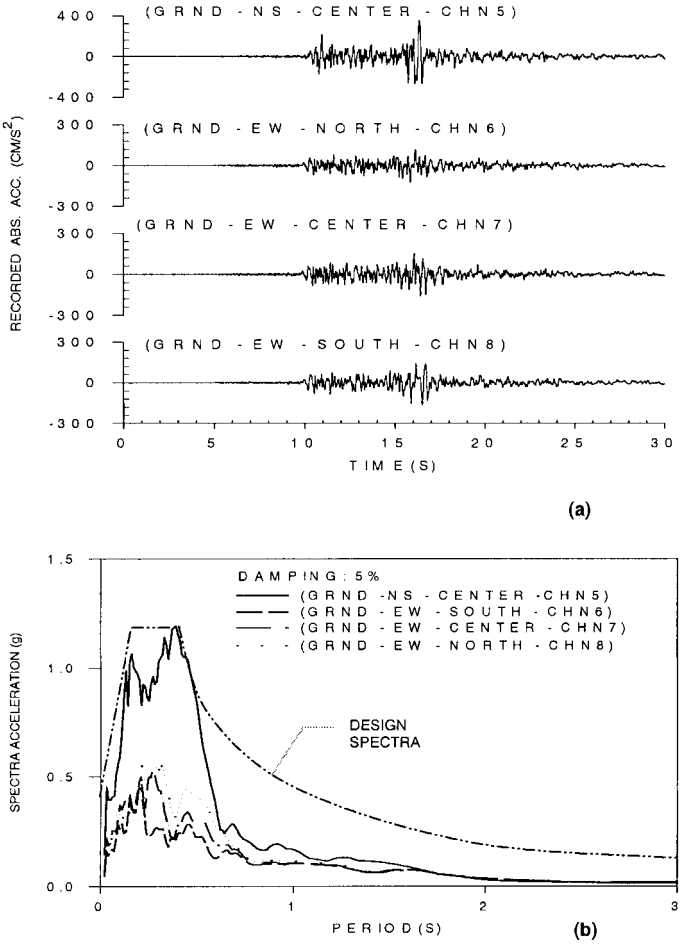

FIG. 2. (a) Recorded Ground Acceleration Time Histories during Northridge Earthquake; (b) Acceleration Response Spectra at Ground/Foundation Level

TABLE 1. Recorded Peak Values of Response in EW and NS Directions

CHN (1)	Acceleration (*g*) (2)
(a) EW	
6	0.13
7	0.16
8	0.17
10	0.07
11	0.07
12	0.14
15	0.08
19	0.14
22	0.15
23	0.16
24	0.19
(b) NS	
5	0.37
9	0.13
13	0.10
17	0.11
21	0.21
25	0.49

Note: Refer to Fig. 1(a) for sensor locations.

velocity, and displacement vectors, respectively, relative to the base; $\ddot{\mathbf{u}}_b$ = vector of base acceleration relative to the ground; and $\ddot{\mathbf{u}}_g$ = vector of ground acceleration.

The equations of motion for the base are as follows:

$$\mathbf{R}^T\mathbf{M}[\ddot{\mathbf{u}} + \mathbf{R}(\ddot{\mathbf{u}}_b + \ddot{\mathbf{u}}_g)] + \mathbf{M}_b(\ddot{\mathbf{u}}_b + \ddot{\mathbf{u}}_g) + \mathbf{C}_b\dot{\mathbf{u}}_b + \mathbf{K}_b\mathbf{u}_b + \mathbf{f} = 0 \tag{2}$$

in which $\mathbf{M}_b$ = diagonal mass matrix of the rigid base; $\mathbf{C}_b$ = resultant damping matrix of viscous isolation elements; $\mathbf{K}_b$ = resultant stiffness matrix of elastic isolation elements; and $\mathbf{f}$ = vector containing the forces mobilized in the nonlinear isolation elements. Employing modal reduction

$$\mathbf{u} = \boldsymbol{\phi}\mathbf{u}^* \tag{3}$$

in which $\boldsymbol{\phi}$ = modal matrix of the fixed-based superstructure, normalized with respect to the mass matrix; and $\mathbf{u}^*$ = modal displacement vector relative to the base. Combining (1)–(3), the following matrix equation is obtained:

$$\begin{bmatrix} \boldsymbol{\phi}^T\mathbf{M}\boldsymbol{\phi} & \boldsymbol{\phi}^T\mathbf{M}\mathbf{R} \\ \mathbf{R}^T\mathbf{M}\boldsymbol{\phi} & \mathbf{R}^T\mathbf{M}\mathbf{R} + \mathbf{M}_b \end{bmatrix} \begin{Bmatrix} \ddot{\mathbf{u}}^* \\ \ddot{\mathbf{u}}_b \end{Bmatrix} + \begin{bmatrix} \boldsymbol{\phi}^T\mathbf{C}\boldsymbol{\phi} & \mathbf{0} \\ \mathbf{0} & \mathbf{C}_b \end{bmatrix} \begin{Bmatrix} \dot{\mathbf{u}}^* \\ \dot{\mathbf{u}}_b \end{Bmatrix}$$

$$+ \begin{bmatrix} \boldsymbol{\phi}^T\mathbf{K}\boldsymbol{\phi} & \mathbf{0} \\ \mathbf{0} & \mathbf{K}_b \end{bmatrix} \begin{Bmatrix} \mathbf{u}^* \\ \mathbf{u}_b \end{Bmatrix} + \begin{Bmatrix} \mathbf{0} \\ \mathbf{f} \end{Bmatrix} = -\begin{bmatrix} \boldsymbol{\phi}^T\mathbf{M}\mathbf{R} \\ \mathbf{R}^T\mathbf{M}\mathbf{R} + \mathbf{M}_b \end{bmatrix} \ddot{\mathbf{u}}_g \tag{4}$$

Because the modal matrix $\boldsymbol{\phi}$ is normalized with respect to mass, the following diagonal matrices are obtained: $\boldsymbol{\phi}^T\mathbf{M}\boldsymbol{\phi} = \mathbf{I}$, $\boldsymbol{\phi}^T\mathbf{K}\boldsymbol{\phi} = \boldsymbol{\omega}^2$, and $\boldsymbol{\phi}^T\mathbf{C}\boldsymbol{\phi} = 2\boldsymbol{\zeta}\boldsymbol{\omega}$, where $\boldsymbol{\omega}$ = diagonal matrix of natural frequencies of the fixed-base structure and $\boldsymbol{\zeta}$ = diagonal matrix of damping ratios of the fixed-base structure.

The forces $\mathbf{f}$ mobilized in the elastomeric isolation bearings are modeled using a smooth hysteretic model [Fig. 1(c)]. Biaxial forces F_x and F_y mobilized during motion along the *x*- and *y*-directions, respectively, of the elastomeric bearing are given by

$$F_x = \alpha \frac{F^y}{D^y} U_x + (1 - \alpha)F^y Z_x \tag{5a}$$

$$F_y = \alpha \frac{F^y}{D^y} U_y + (1 - \alpha)F^y Z_y \tag{5b}$$

in which α = postyielding to preyielding stiffness ratio; F^y = yield force; and D^y = yield displacement [refer to Fig. 1(c)]. The bearing parameters used in the current study are shown in Table 2 (DIS 1989). The variables Z_x and Z_y are dimensionless and governed by the following differential equations, which were proposed by Park et al. (1986):

$$D^y\dot{Z}_x + \gamma|\dot{U}_xZ_x|Z_x + \beta\dot{U}_xZ_x^2 + \gamma|\dot{U}_yZ_y|Z_x + \beta\dot{U}_yZ_xZ_y - A\dot{U}_x = 0 \tag{6}$$

$$D^y\dot{Z}_y + \gamma|\dot{U}_yZ_y|Z_y + \beta\dot{U}_yZ_y^2 + \gamma|\dot{U}_xZ_x|Z_y + \beta\dot{U}_xZ_yZ_x - A\dot{U}_y = 0 \tag{7}$$

Parameters A, β, and γ are dimensionless—$A/(\beta + \gamma) = 1$ is chosen—and U_x, U_y and $\dot{U}_x$, $\dot{U}_y$ represent the displacements and velocities, respectively, that occur at the isolation bearing. It also can be shown that the interaction curve of this biaxial model is circular.

Eqs. (4)–(7) are solved using an efficient pseudoforce solution algorithm (Nagarajaiah et al. 1991a,b). In the pseudoforce method, the forces $\mathbf{f}$ in the nonlinear elastomeric bearings in (4) are moved to the right-hand side of the equations of motion and solved by iteration until convergence is reached. The formulation and solution algorithm have been implemented in the widely used computer program 3D-BASIS (Nagarajaiah et al. 1991a,b) for analyzing base-isolated structures.

A detailed 3D model of the fixed-base superstructure is developed with a rigid floor slab assumption. The superstructure properties, such as beam, column, bracing, and floor slab details, used for analytical modeling are computed from building drawings provided by CSMIP. Three master DOF at the center of mass of each floor are used in the condensed model; hence,

TABLE 2. Properties of Bearings

Property (1)	Lead-Rubber Bearing (2)	Lead-Rubber Bearing (3)	Elastomeric Bearing (4)	Elastomeric Bearing (5)
Base displacement [cm (in.)]	2.8 (1.1)	26.04 (10.25)	2.8 (1.1)	26.04 (10.25)
Yield force F^y [kN (kip)]	80.06 (18.0)	169.02 (38.0)	—	—
Yield displacement D^y [cm (in.)]	0.86 (0.34)	4.83 (1.9)	—	—
Postyield stiffness $\alpha F^y/D^y$ [MN/m (kip/in.)]	2.101 (12.0)	0.718 (4.1)	—	—
Effective stiffness [MN/m (kip/in.)]	4.325 (24.7)	1.247 (7.12)	2.977 (17)	1.576 (9)

Note: Refer to Fig. 1(c) for smooth bilinear hysteretic model.

TABLE 3. Computed and Identified Periods of USC Hospital Building—Fixed-Base Case

	COMPUTED			IDENTIFIED			
	EW	NS	Torsion	EW		NS	
Mode (1)	T (s) (2)	T (s) (3)	T (s) (4)	T (s) (5)	ξ (%) (6)	T (s) (7)	ξ (%) (8)
1	0.92	0.82	0.62	0.92	0.02	0.76	0.03
2	0.37	0.35	0.28	0.37	0.02	0.34	0.03
3	0.2	0.18	0.16	0.2	0.04	0.22	0.05

TABLE 4. Computed and Identified Periods of USC Hospital Building—Base-Isolated Case

	COMPUTED			IDENTIFIED			
	EW	NS	Torsion	EW		NS	
Mode (1)	T (s) (2)	T (s) (3)	T (s) (4)	T (s) (5)	ξ (%) (6)	T (s) (7)	ξ (%) (8)
1	1.25	1.37	1.09	1.32	0.15	1.38	0.13
2	0.55	0.51	0.45	0.51	0.17	0.53	0.14
3	0.26	0.25	0.21	0.27	0.07	0.25	0.05

only 24 DOF (8 floors × 3 DOF per floor) are retained for modeling the USC hospital building in a fixed-base condition. Eigenvalues and eigenvectors of the condensed fixed-base model are used for modeling the superstructure in (4). The computed periods T_n for the first nine modes in the fixed-base condition are shown in Table 3. The damping ratio ξ is assumed to be 5% in all modes.

The prototype bearing tests for the USC hospital building performed by DIS (1989) at various amplitudes is available and is used to extract (Nagarajaiah and Sun 2000) bearing properties. The available bearing test results (DIS 1989), in the form of nonlinear force-displacement loops, are used in this study for explicitly modeling all 68 lead-rubber bearings and 81 elastomeric bearings. The smooth bilinear hysteretic force-displacement loop properties of lead-rubber bearings are shown in Table 2 (DIS 1989; Nagarajaiah and Sun 2000). These properties are the bilinear hysteretic properties [(5)–(7)] of the lead-rubber bearings at 2.8-cm (1.1-in.) displacement (average displacement of CHN9 and CHN11 experienced by the bearings in the Northridge earthquake). Elastomeric bearings are modeled using equivalent linear properties (DIS 1989), shown in Table 2 (DIS 1989; Nagarajaiah and Sun 2000)—lateral stiffness of 2.977 MN/m (17 kip/in.) at 2.8-cm (1.1-in.) displacement and an estimated damping of 3%. The properties of lead-rubber bearings and elastomeric bearings at the maximum displacement of 26.04 cm (10.25 in.) also are shown in Table 3. Note that the values for 2.8 and 26.04 cm are different due to the strain dependency of properties, as shown in the smooth bilinear hysteretic force-displacement loops in Fig. 1(c).

The combined analytical model comprising the superstructure and the isolation system is developed using (4). The response to the Northridge earthquake is computed using the computer program 3D-BASIS (Nagarajaiah et al. 1991a,b).

SYSTEM IDENTIFICATION

The actual dynamic characteristics of the building existing during the Northridge earthquake are estimated based on the identified and recorded transfer functions (Nagarajaiah 1999) obtained from recorded input and output responses. The analytical model is verified by comparing the computed and identified periods/damping ratios. This is necessary due to different dynamic properties used by Asher et al. (1995) to study the response of the USC hospital building. In the analytical model used by Asher et al. (1995), the superstructure was stiffened by two times its original stiffness to match the recorded and computed responses. Such structural stiffness modifications need verification. For the purpose of verification, using linear system identification techniques, a detailed 3D linear model of the base-isolated structure is developed with a rigid floor slab assumption. In the condensed linear model, 27 DOF (9 floors × 3 DOF per floor) are retained for modeling the USC hospital building. Equivalent linear properties extracted from the test results (DIS 1989) of lead-rubber bearings and elastomeric bearings, shown in Table 2, are used for modeling the bearings. Because damping is nonclassical, complex eigenvalue analysis is necessary. However, good estimates of the periods can be obtained by classical eigenvalue analysis. The periods of the base-isolated structure with a linear superstructure and equivalent linear isolation system for the first three modes in the EW, NS, and torsional directions are shown in Table 4. Corresponding periods if the structure were to be fixed base are shown in Table 3. Note that the periods presented are for the structure without any stiffening. Parametric identification methods (Ljung 1987) are used to obtain periods and damping ratios from the transfer functions obtained using nonparametric methods (Ljung 1987) and recorded input and output responses.

Parametric Identification

A linear dynamic system can be described by a constant coefficient linear difference equation

$$\sum_{k=0}^{na} a(k)y(n-k) = \sum_{k=0}^{nb} b(k)x(n-k) \tag{8}$$

where $x(n)$ and $y(n)$ = input and output, respectively. The constant parameters $a(0), \ldots, a(na)$ and $b(0), \ldots, b(nb)$ characterize the linear system. Taking the z transform of (8)

$$Y(z)\sum_{k=0}^{na} a(k)z^{-k} = X(z)\sum_{k=0}^{nb} b(k)z^{-k} \tag{9}$$

where $z = e^{sT} = e^{(\sigma \pm iw)T}$, the system transfer function $H(z)$ relating input and output is

$$H(z) = \frac{Y(z)}{X(z)} = \frac{\sum_{k=0}^{nb} b(k)z^{-k}}{\sum_{k=0}^{na} a(k)z^{-k}} \tag{10}$$

The roots of the denominator polynomial are the poles of $H(z)$. The roots of the numerator polynomial are zeros of $H(z)$. For a stable system, all poles must have a magnitude <1 and should be located within the unit circle. The jth pole of $H(z)$ is given by

$$z_j = \exp[(-\xi_j\omega_j \pm i\omega_j\sqrt{1 - \xi_j^2})\Delta T] \tag{11}$$

where ΔT = sampling interval; and ω_j and ξ_j = frequency and damping ratio of the jth mode of vibration. The frequency and damping ratio can be determined as follows:

$$\omega_j = \frac{1}{\Delta T}\sqrt{\ln^2 r_j + \theta_j^2} \tag{12}$$

$$\xi_j = -\frac{\ln r_j}{\sqrt{\ln^2 r_j + \theta_j^2}} \tag{13}$$

where $r_j = |z_j|$, the magnitude; and $\theta_j = \tan^{-1}[\text{Im}g(z_j)/\text{Re}\ (z_j)]$, the phase angle of the jth pole. The poles are in complex conjugate pairs; hence, the number of identifiable modes is equal to $na/2$.

Nonparametric Identification

The power spectral density (PSD) P_{xx} obtained from the z transform of autocorrelation is related to the cross-spectral density (CSD) P_{xy} obtained from the z transform of cross correlation as follows (Ljung 1987):

$$P_{xy}(z) = H(z^{-1})P_{xx}(z) \tag{14}$$

which also can be written as a function of ω

$$P_{xy}(\omega) = H(\omega)P_{xx}(\omega) \tag{15}$$

The acceleration transfer function estimate is obtained using PSD and CSD. Hanning window is applied to sections and modified periodograms are computed. An average of four modified periodograms are adopted for computing PSD and CSD and for estimating transfer functions. Additional averaging would reduce the variance of the estimate; however, four averages are found to be sufficiently accurate. An overlap length of half the section length is used to reduce the variance of the estimate. Parametric modeling is performed using (10) with na = 20 and nb = 18. The evaluation of the parameters is based on the minimization of the weighted sum of squares of errors between the absolute magnitudes of the actual and desired frequency response function points.

The poles, frequencies, and damping ratios are obtained from the identified transfer functions (Nagarajaiah 1999). The recorded and identified transfer functions, in magnitude and phase angle form, are presented in Fig. 3. Fig. 3 presents the transfer functions between CHN23/CHN7 and CHN21/CHN5 needed to identify the frequencies and damping ratios of the base-isolated structure. As per (1), the frequencies and damping ratios of the structure if it were fixed base can be estimated by means of transfer functions between CHN23/CHN11 and CHN21/CHN09, shown in Fig. 3. Several peaks in the transfer functions are due to interference/noise and are not considered based on low coherence function values. In the base-isolated case the first two transfer function peaks represent the fundamental mode and the second mode. The identified periods and damping ratios for the first three modes in the EW and NS directions of the base-isolated USC hospital building are presented in Table 4, and the corresponding periods and damping

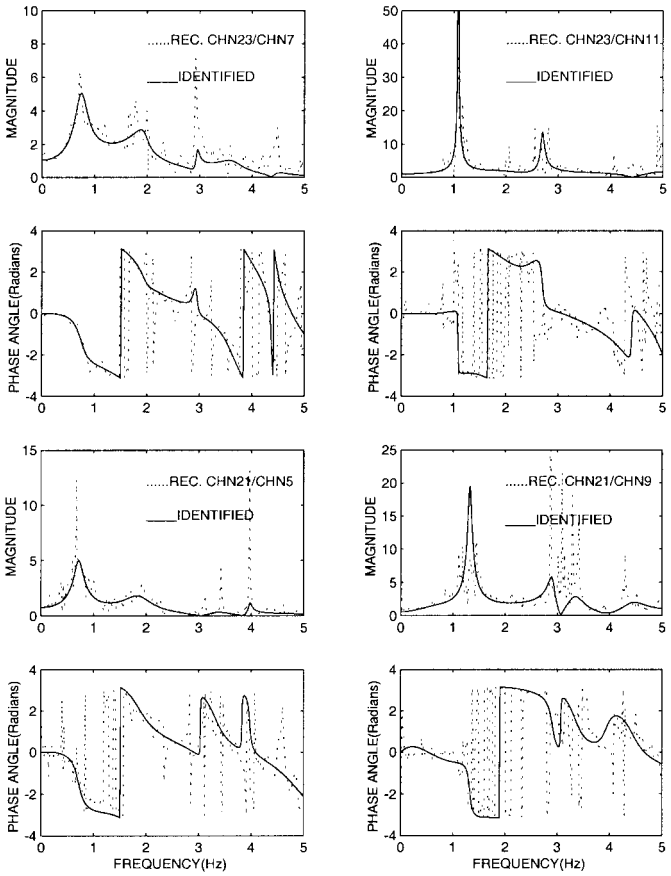

FIG. 3. Recorded and Identified Transfer Functions in EW and NS Directions

ratios for the fixed-base structure are presented in Table 3. Torsional periods could not be reliably identified and hence are not shown in Tables 3 and 4. The comparison between the computed and identified periods indicates that the first and second mode periods differ by about 5–10% in Tables 3 and 4, which is satisfactory. The stiffening of the superstructure adopted by Asher et al. (1995) is not necessary because the computed periods without stiffening are comparable to the actual periods. To compute the damping ratios in the analytical model, a 2D model is obtained by condensing the 3D linear model. Complex eigenvalue analysis using the 2D model [based on the 2D version of (4)], with assumed damping ratios of 5% in the superstructure, 20% in lead-rubber bearings, and 3% in elastomeric bearings estimated from bearing test results (DIS 1989), yields approximately 15, 12, and 6% damping in the first, second, and third mode, respectively (Nagarajaiah and Sun 2000) in the NS and EW directions. The estimated damping values are comparable to those obtained by system identification, except for the second mode damping, which is underestimated.

RESPONSE DURING 1994 NORTHRIDGE EARTHQUAKE

The response of the USC hospital to the Northridge earthquake ground acceleration at CHN5 and CHN7 is computed using the developed 3D-BASIS nonlinear analytical model. Figs. 4 and 5 show a comparison of the recorded and computed responses. The comparison of absolute accelerations and relative displacements [u_i and u_{bi} in (1) and (2)] in the EW and NS directions is satisfactory. The peak displacement of the bearings u_{bi} was 2.25 cm in the EW direction and 3.5 cm in the NS direction. The isolation system yielded [the yield displacement of 0.86 cm (0.34 in.)] and dissipated energy during

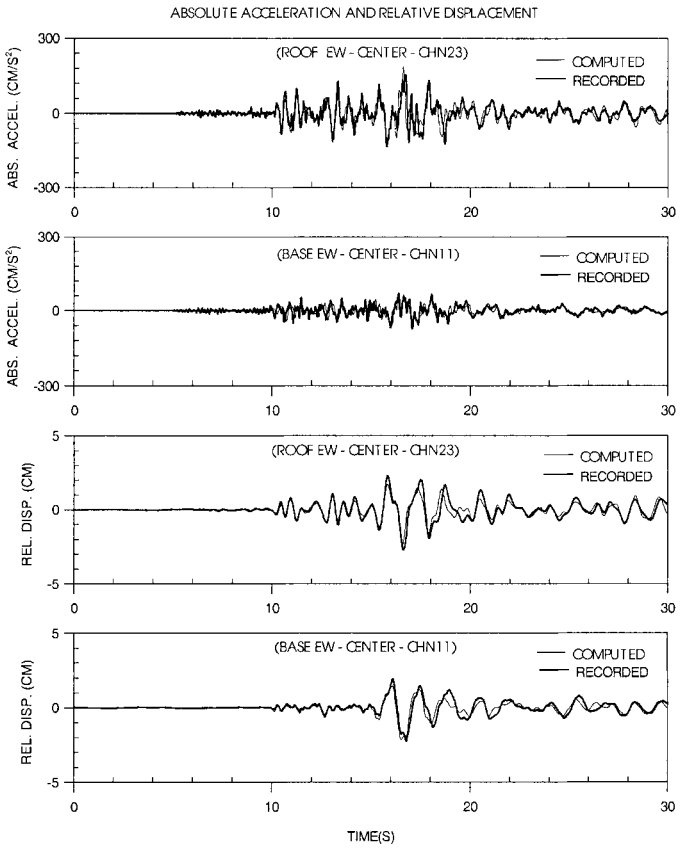

FIG. 4. Comparison of Recorded and Computed Response in Northridge Earthquake in EW Direction (Note: Relative Displacement at Roof Is with Respect to Base and Base Is with Respect to Ground)

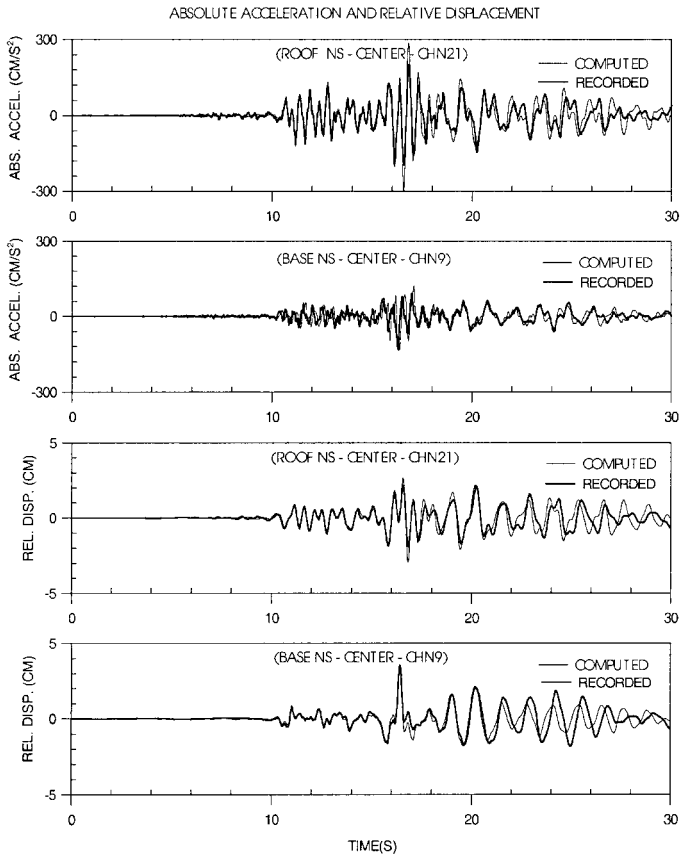

FIG. 5. Comparison of Recorded and Computed Response in Northridge Earthquake in NS Direction (Note: Relative Displacement at Roof Is with Respect to Base and Base Is with Respect to Ground)

a significant portion of the time history. The period of the isolated structure varied due to the bilinear force-displacement behavior of the bearings. The period during the peak cycles of motion was approximately 1.3 s (Table 4). The hysteretic damping in the lead-rubber bearings, estimated from bearing test results (DIS 1989), was approximately 20%. The peak superstructure relative displacement with respect to base [u_i in (1)] was nearly 3 cm. The peak ground acceleration at the center in the EW direction was 0.16g and 0.37g in the NS direction (Table 1). The peak acceleration at the base was 0.07g in the EW direction and 0.13g in the NS direction. The peak acceleration at the roof was 0.16g in the EW direction and 0.21g in the NS direction. The peak roof acceleration was reduced by nearly a factor of 2 (0.21/0.37 $\approx$ 0.56) because of the base-isolation system.

Fig. 6 shows the floor response spectra at the base, fourth floor, sixth floor, and roof for three cases: (1) recorded response; (2) computed response with a bilinear hysteretic model for 68 lead-rubber isolators and a linear model for 81 elastomeric isolators; and (3) computed response with the equivalent linear-isolation system. The spectra of the recorded and computed response in the case with the nonlinear model match well. The response spectra for the case with the linear model do not match as well. The spectral accelerations at the base level, above the isolation system, are <0.5g, as compared to 1.2g ground spectral accelerations, indicating that the isolation system reduced the accelerations and filtered the high frequency vibrations. The response spectra at roof-NS-Center-CHN21 indicates spectral accelerations of 1.1g at 0.5 s (due to second mode response) <1.2g ground spectral accelerations. The spectral accelerations are <0.5g at roof-EW-Center-CHN23. Base isolation reduced spectral accelerations.

Fig. 7 shows the recorded and computed displacement and

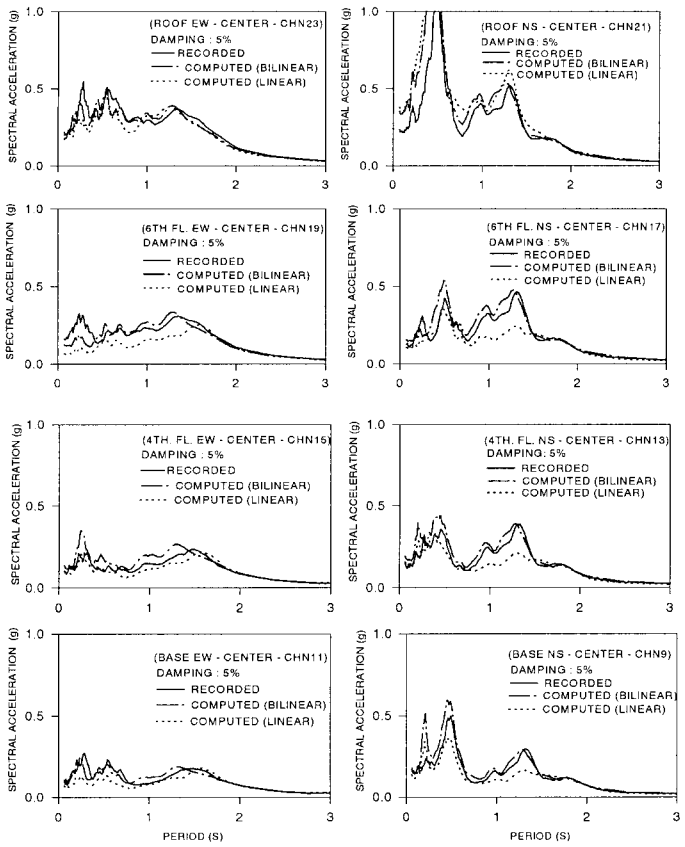

FIG. 6. Recorded and Computed Floor Response Spectra in EW and NS Directions

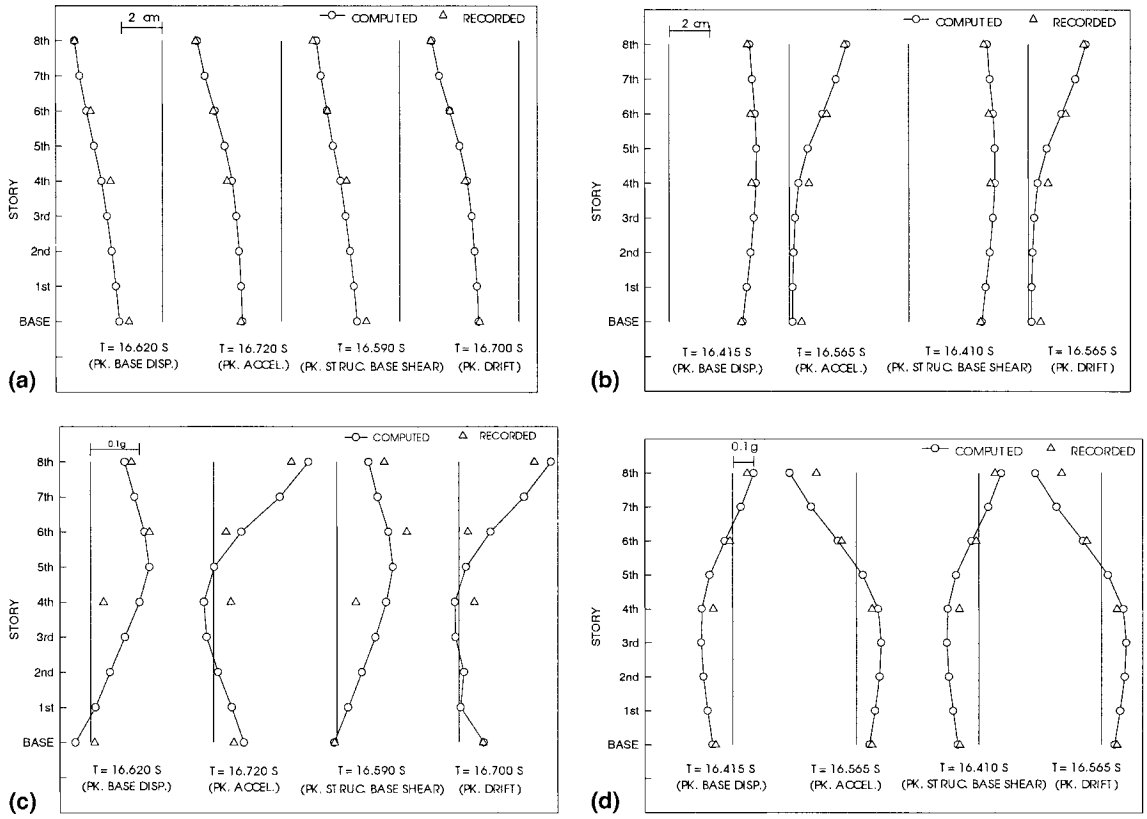

FIG. 7. Recorded and Computed Displacement and Acceleration Profiles: (a) Displacement Profiles—EW Center; (b) Displacement Profiles—NS Center; (c) Acceleration Profiles—EW Center; (d) Acceleration Profiles—NS Center

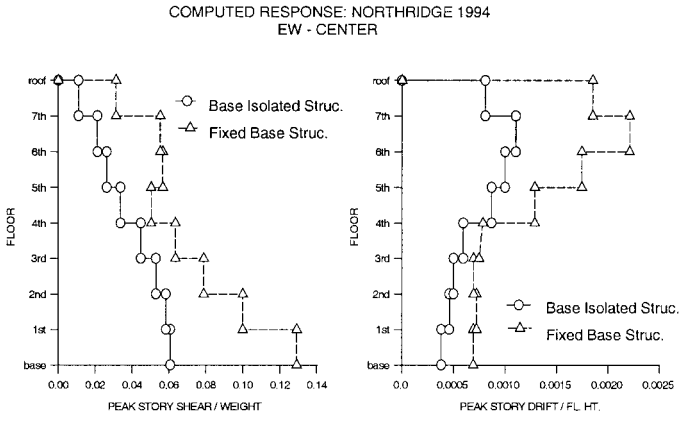

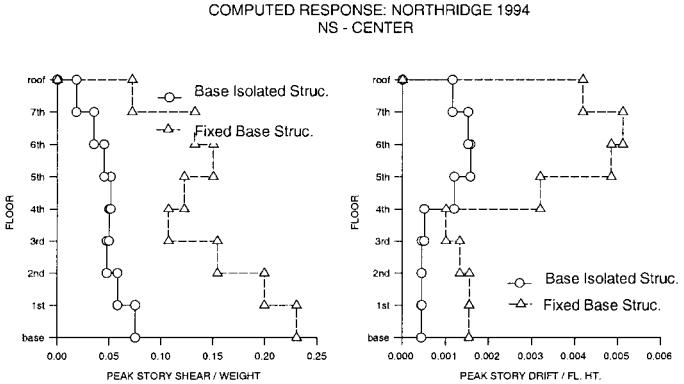

FIG. 8. Comparison between Base-Isolated and Fixed-Base Case: Normalized Peak Story Shear and Drift Envelopes in EW and NS Directions

acceleration profiles in the EW and NS directions at the instants of occurrence of the peak base displacement, peak acceleration, peak structure base shear (above base), and peak drift. The accuracy with which the analytical model captures the displacement response is good, whereas small differences in acceleration response occur in the EW direction. The correlation of the recorded and computed responses demonstrates the accuracy of the nonlinear modeling techniques presented. Displacement profiles in the EW direction are dominated by the first mode, and acceleration profiles involve several modes. When the peak structure base shear occurs in the EW direction, the accelerations ($<0.15g$) and the inertial forces are in phase due to the first mode response. Displacement and acceleration response profiles in the NS direction display combined first and second mode responses. When the peak structure base shear occurs in the NS direction, the accelerations ($<0.2g$) and inertial forces are out of phase due to the second mode, which is beneficial in reducing the base shear.

Fig. 8 shows a comparison between the computed peak response envelopes of the base-isolated USC hospital and the response if the building were to be fixed base. The benefits of seismic isolation become clear by examining the peak story shear and peak story drift envelopes in the EW and NS directions. The superstructure remained elastic in the base-isolated case. The peak drift was nearly 30% of code specifications. However, in the fixed-base case in the NS direction, the peak drift exceeds code specifications. The fixed-base superstructure would experience three times more story shears and drifts than that of the superstructure in the base-isolated case. In the fixed case both first and second modes contribute to the response, with effective mass of 69 and 24%, respectively. The second mode contribution is substantial. This is evident in the displacement and acceleration profiles in the NS direction presented in Fig. 9 (see peak drift and peak acceleration profiles).

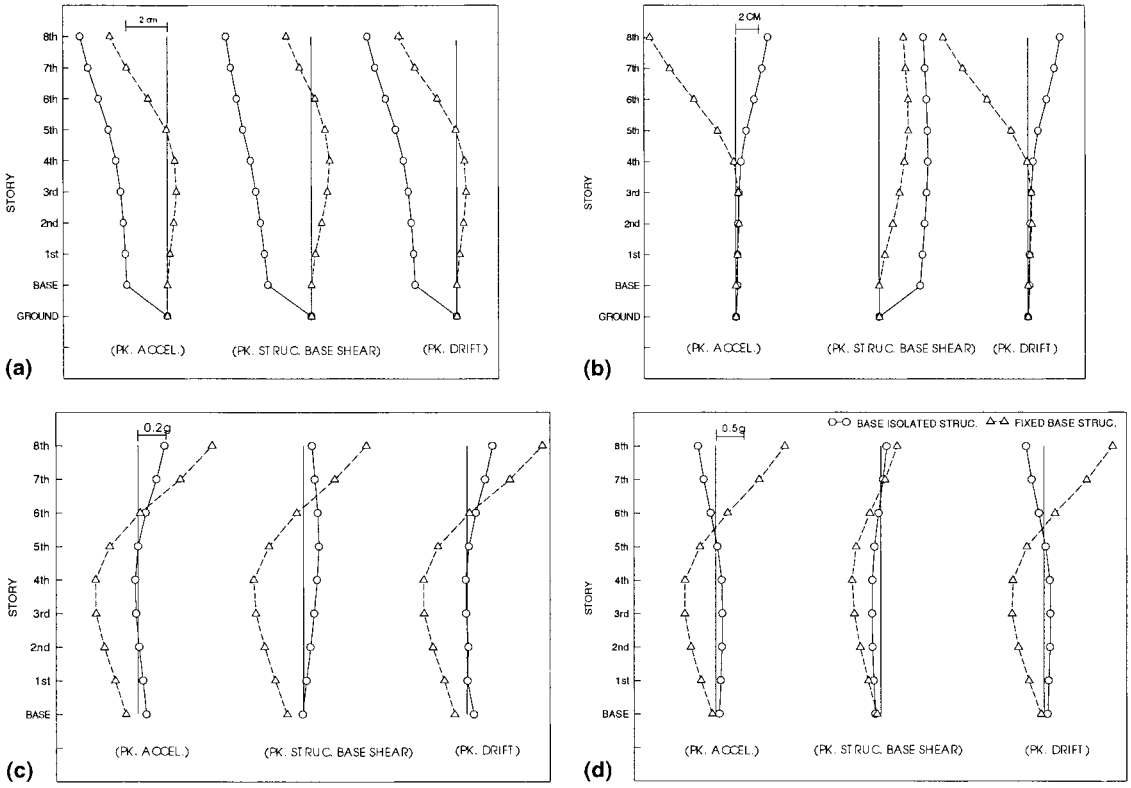

FIG. 9. Comparison between Base-Isolated and Fixed-Base Case: Displacement and Acceleration Profiles: (a) Displacement Profiles—EW Center; (b) Displacement Profiles—NS Center; (c) Acceleration Profiles—EW Center; (d) Acceleration Profiles—NS Center

The profiles in Fig. 9 are at the instants of occurrence of the peak acceleration, peak structure base shear (above base), and peak drift in the base-isolated and fixed-base cases. The changes in stiffness after the fifth floor, because of setbacks, also cause increased response. In the base-isolated case, larger displacement occurs at the base and smaller displacements/drifts occur in the superstructure. In the fixed case larger displacements occur in the superstructure, increasing the drift. In the fixed-base case acceleration profiles, the second mode is dominant and peak acceleration of nearly 1*g* occurs in the NS direction. The following quote from the Earthquake Engineering Research Institute (EERI 1996) is worth noting:

> Workers in a large supply room within the USC hospital reported a gentle swaying motion with no disruption of supplies or materials falling off shelves as a result of the earthquake. In contrast, a pharmacy in an adjacent fixed base medical building reported substantial disruption of the supplies that were placed on shelves.

The maximum flexible floor diaphragm horizontal displacements inferred from the records were of the order of 1.27 cm (0.5 in.), which is negligible compared to the length of the building of 92.35 m (303 ft); hence, no significant flexible diaphragm effects occurred during the earthquake. The torsional response inferred from the records was nominal, with eccentricities of approximately 5% the length of the building. The interested reader is referred to Nagarajaiah and Sun (2000) for further details.

EFFECTIVENESS OF BASE ISOLATION

In this study the USC hospital base-isolated building has been modeled as a nonlinear system. However, considering the modal response of an equivalent linear system provides insight into the reasons for the effectiveness of base isolation during the Northridge earthquake:

- The period lengthening and dominant fundamental mode response are the main reasons for the effectiveness of base isolation. The estimated 15% damping in the fundamental mode reduced the displacement further. The fundamental period in the EW and NS directions was nearly 1.3 s (Table 4) in the base-isolated condition. The fundamental period was beyond the predominant periods of the ground motion spectral accelerations [Fig. 2(b)]. In the fundamental mode, larger displacement occurred at the base with smaller displacements in the superstructure. The fundamental mode dominated the response in the EW direction, as shown in Fig. 7. A significant amount of response occurred in the fundamental mode (effective modal mass 93%) in the NS direction, as shown in Fig. 7. This is also evident in Fig. 10(a), in which the first mode, second mode, and total responses in the NS direction are shown. However, the ground acceleration pulse of a nearly 0.4-s period, between 16.2 and 16.6 s, in the NS direction [CHN5 in Fig. 2(a)] excited the first and second modes, as shown in Fig. 10.
- The second mode in the NS and EW directions, of a 0.5-s period (Table 4), was in the predominant period range of ground motion [Fig. 2(b)]. However, the second mode (effective modal mass 6%) had smaller participation when compared to the fixed-base case (effective modal mass 24%). Increased damping of nearly 17%, as compared to the original 5% damping, was also beneficial. Hence, the second mode response in the NS direction, as shown in Fig. 10(b), was reduced; however, it was not negligible, as is usually the case for base-isolated buildings. The total relative roof displacement response—combined response of modes 1 and 2 in the NS direction—is shown in Fig. 10(c) and compares favorably with Fig. 5(c), which was obtained using nonlinear analysis.
- In base-isolated structures, the contribution of the second mode is negligible or orthogonal (Kelly 1993) to the earthquake input and the fundamental mode dominates the

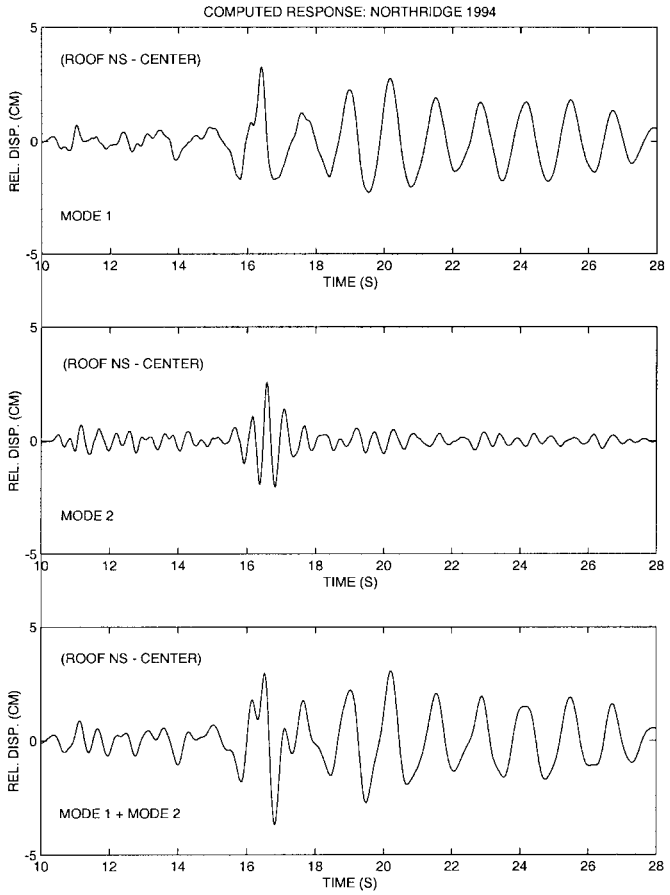

FIG. 10. Computed Linear Response of Modes 1 and 2 in NS Direction

response when the base-isolation system is functioning at design displacement. This and the period lengthening are the main reasons for the effectiveness of base isolation. In the case of the USC hospital, the fundamental period is 2.2 s at a design displacement of 26.04 cm (10.25 in.), obtained using an effective stiffness of 1.247 MN/m (7.12 kip/in.) for lead-rubber bearings and 1.576 MN/m (9 kip/in.) for elastomeric bearings (Table 2). The effective modal mass for the first and second mode is 99.5 and 0.47%, respectively. Hence, the total response would be dominated by the first mode and the second mode response would be negligible or orthogonal to the earthquake.

The bearing displacement (3.5 cm) during the Northridge earthquake was only 13.5% of the design displacement [26.04 cm (10.25 in.)]. This is because ground spectral acceleration at the fundamental period (1.3 s) was only 30% of design spectral acceleration [Fig. 2(b)]. The isolation gap provided by the designers (Asher et al. 1995) is 26.04 cm (10.25 in.) [Fig. 2(b)]. In this study, to assess the response under the design earthquake, the peak displacement is estimated using the developed nonlinear analytical model with isolator properties at 26.04 cm (Table 2). An artificially generated design spectrum compatible ground motion is used as the excitation. The computed peak base displacement is nearly 15 cm, which is less than the isolation gap.

CONCLUSIONS

The seismic response and performance evaluation of the base-isolated USC hospital building has been presented. It is evident from the evaluation that the USC hospital performed well and base isolation was effective in reducing the response and providing earthquake protection. The main conclusions of the study are

- The period lengthening and dominant fundamental mode response are the main reasons for the effectiveness of base isolation. The estimated 15% damping in the fundamental mode reduced the displacement further.
- The Northridge earthquake had significant energy in the higher mode range but could not transmit the energy because the participation of higher modes was reduced due to base isolation.
- Base isolation reduced the base shear, accelerations, and story drifts. The peak roof acceleration was reduced to nearly 50% of the peak ground acceleration due to the effectiveness of base isolation. The peak drift was <30% of the code specification, and the superstructure was elastic.
- Comparison of the computed response in the base-isolated case and the corresponding case if the structure were fixed base indicates that the response would have been three times larger in the fixed-base case.
- The bearing displacement during the Northridge earthquake was only 13.5% of the design displacement [26.04 cm (10.25 in.)]. This is because ground spectral acceleration at the fundamental period was only 30% of design spectral acceleration. In this study the computed peak base displacement in the case of an earthquake with spectral accelerations at 2.2 s equal to the design spectra is 15 cm, which is less than design displacement. Hence, the building is expected to perform well in future earthquakes similar to those used in the original design.

The results of the analytical model and the system identification are in good agreement, indicating the accuracy of the developed model and the modeling techniques. The system identification can be used to reliably estimate the dynamic characteristics of base-isolated buildings and also to estimate the energy dissipation capacity of the base-isolation system. The comparisons between the computed and recorded responses demonstrate the accuracy of the presented analytical modeling techniques used in 3D-BASIS (Nagarajaiah et al. 1991a,b), which is extensively used in the analysis and design of base-isolated structures.

ACKNOWLEDGMENTS

Funding provided for this study by the CSMIP (Contract No. 1093-556) is gratefully acknowledged. Thanks go to Drs. M. Huang, G. Maldonado, R. G. Darragh, and A. F. Shakal of CSMIP for providing building drawings, bearing test results, and recorded data.

APPENDIX. REFERENCES

Asher, J. W., Hoskere, S., Ewing, R., Van Volkinburg, D. R., Mayes, R., and Button, M. (1995). ''Seismic performance of the base isolated USC university hospital in the 1994 Northridge earthquake.'' *Proc., ASME Pressure Vessels and Piping Conf., Vol. 319*, New York, 147–154.

Dynamic Isolation Systems (DIS). (1989). ''Test results for seismic isolation bearings for the USC university hospital building.'' *Rep. No. 5822-68*, Calif.

Earthquake Engineering Research Institute (EERI). (1996). ''Northridge earthquake of January 17, 1994.'' *Earthquake spectra*, 2, 248.

Kelly, J. M. (1993). *Earthquake resistant design with rubber*, 1st Ed., Springer, New York.

Ljung, L. (1987). *System identification*, Prentice-Hall, Englewood Cliffs, N.J.

Nagarajaiah, S. (1999). ''System identification of base isolated USC hospital building from recorded response.'' *Proc., 17th Int. Modal Anal. Conf.*, SEM, Fla., 159–165.

Nagarajaiah, S., Reinhorn, A. M., and Constantinou, M. C. (1991a). ''3D-BASIS: Nonlinear dynamic analysis of three dimensional base isolated structures—Part II.'' *Rep. No. NCEER-91-0005, Nat. Ctr. for Earthquake Engrg. Res.*, State University of New York, Buffalo.

Nagarajaiah, S., Reinhorn, A. M., and Constantinou, M. C. (1991b). ''Nonlinear dynamic analysis of 3-D-base-isolated structures.'' *J. Struct. Engrg.*, ASCE, 117(7), 2035–2054.
Nagarajaiah, S., and Sun, X. (1995). ''Response of base isolated buildings during the 1994 Northridge earthquake.'' *Proc., SMIP95 Seminar*, 41–55.
Nagarajaiah, S., and Sun, X. (2000). ''Response of base isolated buildings in the 1994 Northridge earthquake.'' *Rep. No. 51*, Rice University, Houston.
Park, Y. J., Wen, Y. K., and Ang, A. H. S. (1986). ''Random vibration of hysteretic systems under bi-directional ground motions.'' *Earthquake Engrg. Struct. Dyn.*, 14(4), 543–557.
Shakal, A., et al. (1994). ''CSMIP strong motion records from the Northridge earthquake of 17 January 1994.'' *Rep. No. OSMS 94-07*, Calif. Strong Motion Instrumentation Program, California Department of Conservation, Calif.
Wilson, E. L., Hollings, J. P., and Dovey, H. H. (1975). ''ETABS—Three dimensional analysis of building systems.'' *Rep. No. UCB/EERC—75/13*, Earthquake Engrg. Res. Ctr., University of California, Berkeley, Calif.